VERSITA

Cent. Eur. J. Chem. • 11(6) • 2013 • 920-926
DOI: 10.2478/s11532-013-0235-2

Central European Journal of **Chemistry**

Preparation, characterization and photocatalytic activity of $Co_3O_4/LiNbO_3$ composite

Research Article

Beata Zielinska[1*], Magdalena Janus[2], Ryszard J. Kalenczuk[1]

[1]*Institute of Chemical and Environment Engineering, West Pomeranian University of Technology, Szczecin 70-322 Szczecin, Poland*

[2]*Department of Sanitary Engineering, West Pomeranian University of Technology, Szczecin 70-310 Szczecin, Poland*

Received 26 October 2012; Accepted 10 January 2013

Abstract: The $Co_3O_4/LiNbO_3$ composites were synthesized by impregnation of $LiNbO_3$ in an aqueous solution of cobalt nitrate and next by calcination at 400°C. The activity of produced samples has been investigated in the reaction of photocatalytic hydrogen generation. The crystallographic phases, optical and vibronic properties were studied using X-ray diffraction (XRD), diffuse reflectance (DR) UV–vis and resonance Raman spectroscopic techniques, respectively. The influence of cobalt content (range from 0.5 wt.% to 4 wt.%) on the photocatalytic activity of $Co_3O_4/LiNbO_3$ composites for photocatalytic hydrogen generation has been investigated. $Co_3O_4/LiNbO_3$ composites exhibited higher than $LiNbO_3$ photocatalytic activity for hydrogen generation. The highest H_2 evolution efficiency was observed for $Co_3O_4/LiNbO_3$ composite with 3 wt.% cobalt content. The amount of H_2 obtained in the presence of $LiNbO_3$ and $Co_3O_4/LiNbO_3$ (3 wt.% of cobalt content) was 1.38 μmol/min and 2.59 μmol min^{-1}, respectively.

Keywords: *$LiNbO_3$, Co_3O_4 • Photocatalysis • Hydrogen generation*

1. Introduction

Alkali niobates, such as lithium niobate ($LiNbO_3$), sodium niobate ($NaNbO_3$) and potassium niobate ($KNbO_3$) crystals have received great attention due to their outstanding ferroelectric, piezoelectric, photorefractive, acoustic-optical, electro-optical, nonlinear optical properties and their superior mechanical and chemical stability [1]. Among alkali niobates, lithium niobate ($LiNbO_3$) is one of the most important compounds. At room temperature, $LiNbO_3$ is one of the ferroelectric crystalline materials which has the largest spontaneous polarization [1-2]. Moreover, with regard to its excellent ferroelectric features $LiNbO_3$ is a popular piezoelectric and dielectric material in many systems [1]. On the other hand, $LiNbO_3$ can be a photocatalyst for the photocatalytic reactions [3-6]. For example, QY. Chen *et al.* [3] stated that $LiNbO_3$ prepared by conventional solid state reaction was active in the reaction of photocatalytic hydrogen evolution from aqueous methanol solution. Saito *et al.* [4] reported that $LiNbO_3$ nanowires produced *via* metal complex-based method exhibited good photocatalytic properties for overall water splitting. The authors also stated that $LiNbO_3$ nanowires showed enhanced photocatalytic properties as compared with a bulky $LiNbO_3$ synthesized by a solid state reaction. In our previous work [5], we presented the study showing that lithium niobates based catalyst without any further modification or doping can be applied as photocatalyst for hydrogen generation. The results indicated that the most active catalyst for the photocatalytic generation of hydrogen is the one containing two lithium niobate phases such as $LiNbO_3$ and $LiNb_3O_8$. Furthermore, M. Stock *et al.* [6] studied the photocatalytic activity of $LiNbO_3$ and Fe and Mg doped $LiNbO_3$ in the reaction of Acid Black 1 and Rhodamine B decomposition under solar illumination. In this study, the authors point out that lithium niobate is a reactive photocatalyst under solar irradiation and Mg doped

* E-mail: bzielinska@zut.edu.pl

$LiNbO_3$ exhibits higher photocatalytic activity than pure $LiNbO_3$.

It is known that to obtain high photocatalytic active photocatalyst in the reaction of hydrogen generation, it is essential to load metals or metal oxides on the surface of photocatalyst. The loaded metal (Pt, Ru) or metal oxides (NiO, Co_3O_4, CuO) can capture the photogenerated electrons reducing the electron-hole recombination and act as reaction sites for the reduction of H^+ [7-8]. It is known that one of the best oxides that enhances the photocatalytic activity of photocatalysts is NiO [9-12]. For example, the photocatalytic water splitting in the presence of many different tantalates was studied by Kudo [11]. The author stated that loading a NiO co-catalyst, which works as active sites for proton reduction, significantly improves the photocatalytic activity of tantalates. The amount of evolved hydrogen produced over $NaTaO_3$ and $NiO/NaTaO_3$ (0.05 mass% of NiO) was 160 and 2180 μmol h^{-1}, respectively.

In the current study, the efficiency of Co_3O_4 loaded $LiNbO_3$ as photocatalyst in the reaction of photocatalytic hydrogen generation will be presented. The influence of cobalt content on the photocatalytic activity of $Co_3O_4/LiNbO_3$ composites for photocatalytic hydrogen generation has been investigated. The photocatalytic reactions were carried out in the presence of formic acid.

2. Experimental procedure

2.1. Materials

Niobium pentaoxide (Nb_2O_5, purity 99.99%, Aldrich), lithium hydroxide (LiOH□H_2O, purity 98%, Sigma-Aldrich) and cobalt nitrate ($Co(NO_3)_2$•$6H_2O$, purity 98%, Sigma-Aldrich) were used as the starting materials for the synthesis of $LiNbO_3$ and $Co_3O_4/LiNbO_3$ composites.

2.2. $Co_3O_4/LiNbO_3$ composite preparation

In the $LiNbO_3$ preparation procedure, the two steps synthesis (impregnation and calcination) was applied. The molar ratio of LiOH:Nb_2O_5 was 2:1. The excess amount of lithium hydroxide (10%) was added to compensate the volatilization. The excess of LiOH was washed out with water. In the first step of the $LiNbO_3$ preparation, Nb_2O_5 was impregnated in the aqueous solution of lithium hydroxide. After impregnation the as-obtained material was dried at the temperature of 70°C for 24 hours, and next calcinated at 550°C. The annealing time at the required calcination temperature was fixed to 20 hours.

The $Co_3O_4/LiNbO_3$ composite powders were prepared by an impregnation method from the aqueous solution of cobalt nitrate. The content of loading species is calculated according to the weight percentage of cobalt. The mass content of cobalt metal ions in $LiNbO_3$ was range from 0.5% to 4%. In the first step of the $Co_3O_4/LiNbO_3$ preparation the $LiNbO_3$ and $Co(NO_3)_2$•$6H_2O$ solution were put into a ceramic dish. The obtained suspension was stirred during the evaporation of water. Afterwards, the dried powder was calcinated at the temperature of 400°C for 4 hours. The photocatalysts prepared in the above-mentioned way are labeled as 0.5wt.% - $Co/LiNbO_3$, 1wt.% - $Co/LiNbO_3$, 2wt.% - $Co/LiNbO_3$, 3wt.% - $Co/LiNbO_3$, 4wt.% - $Co/LiNbO_3$.

2.3. Experimental procedure and techniques

The crystallographic structure and the optical properties of the prepared photocatalysts were characterized by X-ray diffraction (XRD) analysis (X'Pert PRO Philips diffractometer, CoK_α radiation) and DR-UV-vis spectroscopy using Jasco (Japan) spectrometer, respectively. Additionally, resonance Raman study was performed using Resonance Raman Renishaw InVia Microscope with laser length 785 nm. Finally, the specific surface areas of catalysts were measured by nitrogen gas adsorption method using Micrometrics ASAP 2010 device.

2.4. Determination of photocatalytic activity

The activities of the obtained photocatalysts was examined *via* the photocatalytic hydrogen generation in the presence of formic acid. The reactions were carried out in a closed system with an inner-irradiation-type reactor. A medium pressure mercury lamp of 150W as a light source was applied. The lamp provided the light of wavelength ranging from 200 nm to 600 nm with the maximum intensity of 366 nm. The reactions were performed with formic acid solution (0.1 mol dm^{-3}) and constant amount of catalysts (0.2 g). Firstly, powder of the photocatalysts was dispersed in 700 cm^3 of aqueous solution of formic acid. Afterwards, the suspension was mixed with a magnetic stirrer for 1 hour in the presence of argon flow to remove oxygen. Finally, the solution was irradiated for 150 minutes without argon purging. The evolved hydrogen was determined using a gas chromatograph (Chrome5) equipped with a thermal conductivity detector (TCD).

3. Results and discussion

Fig. 1 shows a comparison of XRD patterns of original Nb_2O_5 (pattern a) and the material produced after calcination of Nb_2O_5 and LiOH at the temperature of 550°C for 20 hours (pattern b). According to the phase

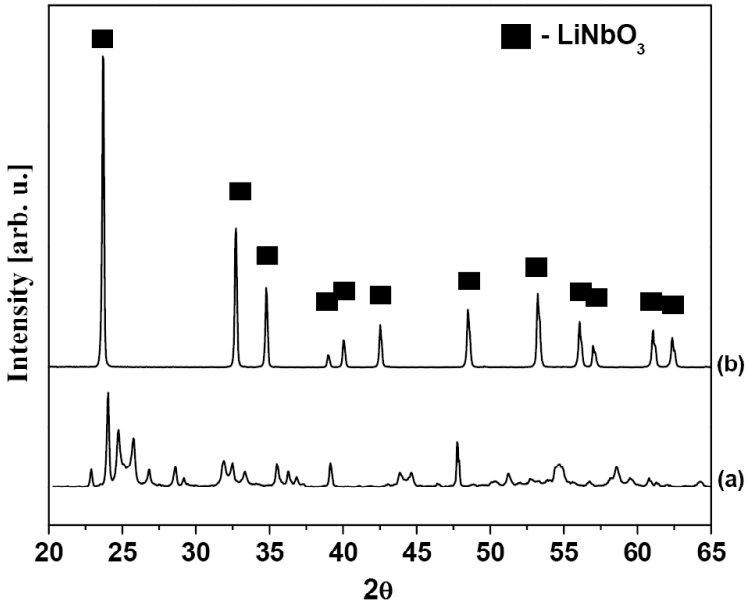

Figure 1. XRD patterns of Nb_2O_5 (a), and material produced after calcination of Nb_2O_5 and LiOH at the temperature of 550°C for 20 hours (b).

analysis the material obtained after the reaction of Nb_2O_5 and LiOH contained lithium niobate at a rhombohedral structure ($LiNbO_3$, JCPDS card no 85-2456). The crystalline structures of all modified photocatalysts have also been analyzed. The XRD patterns of pure $LiNbO_3$ and $Co_3O_4/LiNbO_3$ composites with different Co contents are presented in Fig. 2. No diffraction peaks corresponding to new phase of cobalt oxide are found for $Co_3O_4/LiNbO_3$ composites with cobalt content below 1 wt.% (patterns b). The absence of reflection for deposits could result from low concentration of Co below the detection limit of XRD. However, for cobalt content range from 1 wt.% to 4 wt.%, small diffraction peaks of new phase such as Co_3O_4 (JCPDS card no. 09-0418) next to $LiNbO_3$ have been detected (patterns c-f).

The Raman spectra of the produced $LiNbO_3$ (spectrum a) and $Co_3O_4/LiNbO_3$ composites (spectra b-f) are shown in Fig. 3. Raman spectrum of $LiNbO_3$ shows ten peaks at about 151, 237, 257, 275, 319, 368, 430, 580, 626 and 874 cm^{-1}. For $Co_3O_4/LiNbO_3$ composites all bands, which are characteristic of $LiNbO_3$ have also been observed. Moreover, new clear peaks at 194, 485, 524 and 694 cm^{-1} are detected for the $Co_3O_4/LiNbO_3$ composites. Those peaks correspond to the F_{2g} (194 cm^{-1}), E_g (485 cm^{-1}), F_{2g} (524 cm^{-1}) and A_{1g} (694 cm^{-1}) Raman active modes of Co_3O_4 [13-16]. This is in agreement with the XRD analysis of the samples.

DR-UV-vis spectra were measured to characterize the light absorption ability of the produced photocatalysts. Fig. 4 shows the diffuse reflection spectra of $LiNbO_3$ (spectrum a) and $Co_3O_4/LiNbO_3$ composites with different Co contents (spectra b-f). A single UV absorption edge can be clearly observed for $LiNbO_3$. The band gap energy of the $LiNbO_3$ which was determined with the assistance of the Kubelka–Munk method is 3.86 eV. The estimated value of band gap of produced $LiNbO_3$ is similar to that described in the literature [1,17-18]. Noticeably, the spectra of $Co_3O_4/LiNbO_3$ samples show new visible absorption bands centered at about 450 nm and 750 nm. Those two bands are characteristic of Co_3O_4 [19-21]. Co_3O_4 is a p-type semiconductor with direct transition at 1.45 eV and 2.07 eV which corresponds to O^{2-} - Co^{3+} and O^{2-} - Co^{2+} charge transfer processes, respectively [20].

According to the manufacturer's data, $LiNbO_3$ has a BET surface area of 4.86 $m^2\ g^{-1}$. One could observe that all $Co_3O_4/LiNbO_3$ composite materials have higher BET surface areas than that of $LiNbO_3$. Moreover, BET surface area of the $Co_3O_4/LiNbO_3$ samples increases with an increase Co_3O_4 content in composites. BET surface are of $Co_3O_4/LiNbO_3$ composites is 4.94 $m^2\ g^{-1}$ (0.5 wt.%-Co/$LiNbO_3$), 5.06 $m^2\ g^{-1}$ (1 wt.%-Co/$LiNbO_3$), 5.24 $m^2\ g^{-1}$ (2 wt.%-Co/$LiNbO_3$), 5.28 $m^2\ g^{-1}$ (3 wt.%-Co/$LiNbO_3$) and 5.39 $m^2\ g^{-1}$ (4 wt.%-Co/$LiNbO_3$).

To determine the photocatalytic activity of the synthesized $LiNbO_3$ and $Co_3O_4/LiNbO_3$ composites the photocatalytic hydrogen generation was investigated. The results of hydrogen generation are shown in Fig. 5. The kinetics of the hydrogen generation in the presence of formic acid during the first 150 minutes of UV irradiation can be described by zero order kinetics. The presented results clearly indicate that

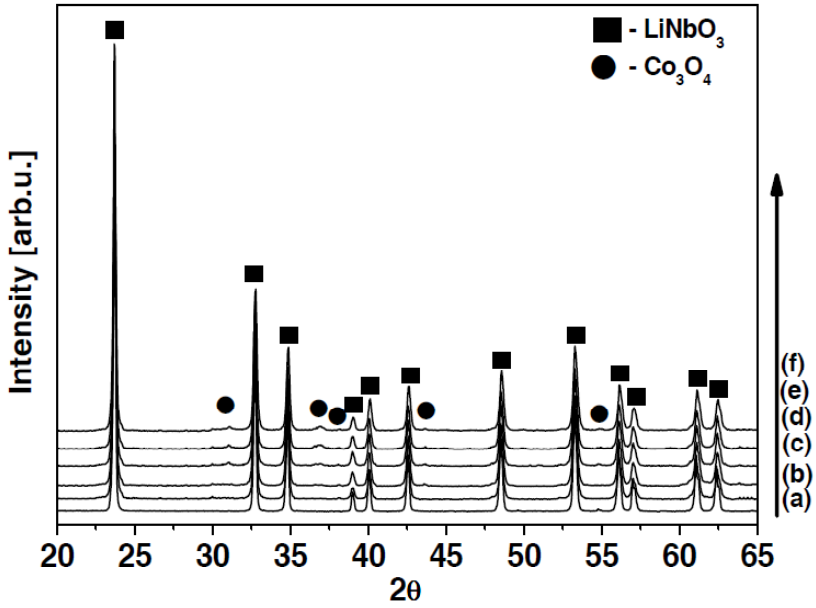

Figure 2. XRD patterns of $LiNbO_3$ (a), 0.5 wt.% -Co/$LiNbO_3$ (b), 1 wt.% -Co/$LiNbO_3$ (c), 2 wt.% -Co/$LiNbO_3$ (d), 3 wt.% -Co/$LiNbO_3$ (e) and 4 wt.% -Co/$LiNbO_3$ (f).

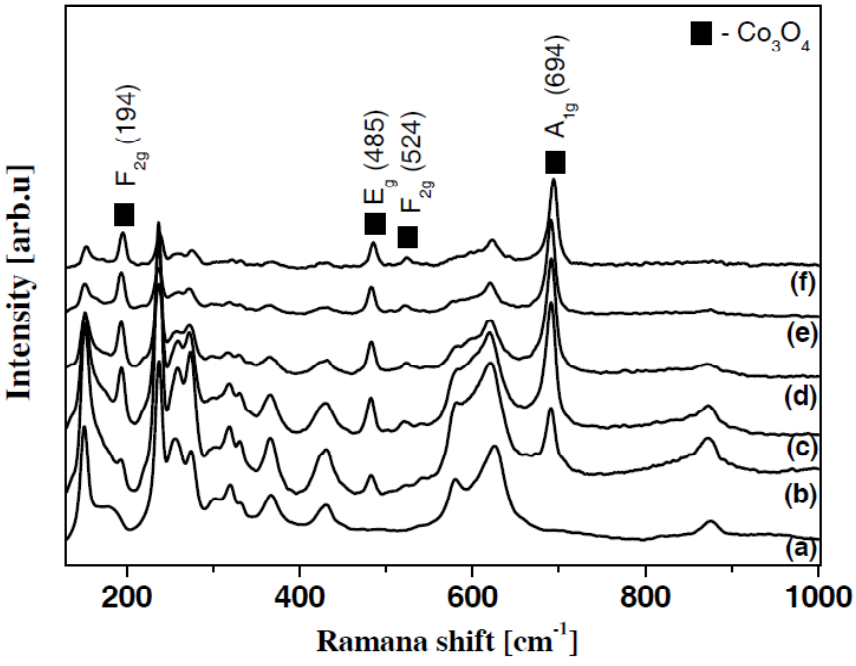

Figure 3. Raman spectra of samples: $LiNbO_3$ (a), 0.5 wt.% -Co/$LiNbO_3$ (b), 1 wt.% -Co/$LiNbO_3$ (c), 2 wt.% -Co/$LiNbO_3$ (d), 3 wt.% -Co/$LiNbO_3$ (e) and 4 wt.% -Co/$LiNbO_3$ (f).

the synthesized $LiNbO_3$ and Co_3O_4/$LiNbO_3$ composites are active photocatalysts in hydrogen generation. In addition, Co_3O_4/$LiNbO_3$ composites exhibited higher than $LiNbO_3$ photocatalytic activity for hydrogen generation. The higher photocatalytic activity of Co_3O_4/$LiNbO_3$ composites can be explained by two effects: (i) higher BET surface area and (ii) the interaction between the base photocatalyst ($LiNbO_3$) and the loaded co-catalyst (Co_3O_4) which might be advantageous in the separation of photogenerated electrons and holes reducing the recombination. Conduction band (CB) and valence band (VB) of the semiconductor at the point of zero charge (pH_{zpc}) can be calculated by the Eq. 1 [20-22]:

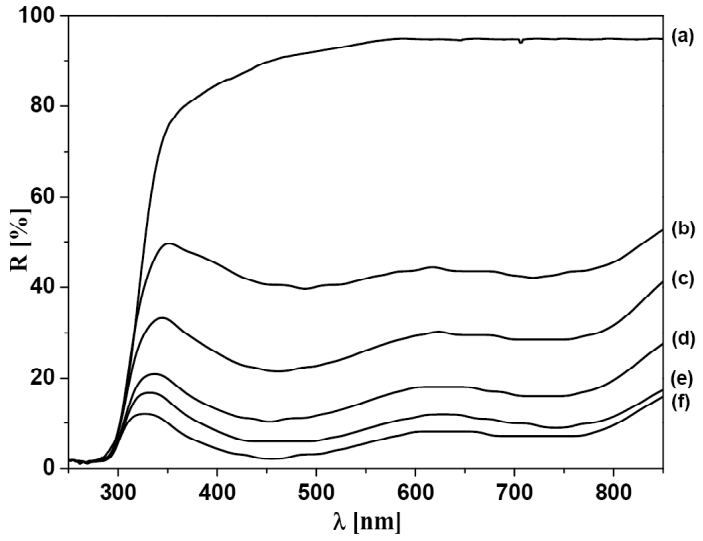

Figure 4. UV-vis spectra of samples: $LiNbO_3$ (a), 0.5 wt.% -Co/$LiNbO_3$ (b), 1 wt.% -Co/$LiNbO_3$ (c), 2 wt.% -Co/$LiNbO_3$ (d), 3 wt.% -Co/$LiNbO_3$ (e) and 4 wt.% -Co/$LiNbO_3$ (f).

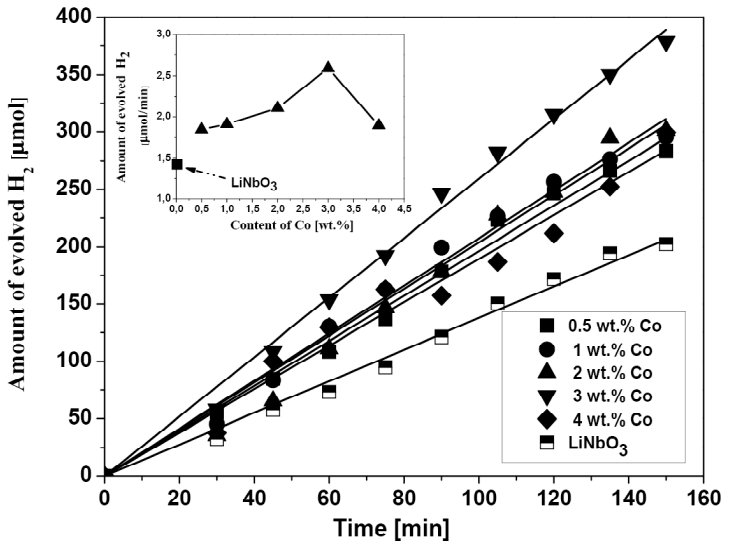

Figure 5. Photocatalytic H_2 evolution of $LiNbO_3$ and $Co_3O_4/LiNbO_3$ composites (HCOOH concentration – 0.1 mol dm^{-3}, amount of catalysts – 0.2 g).

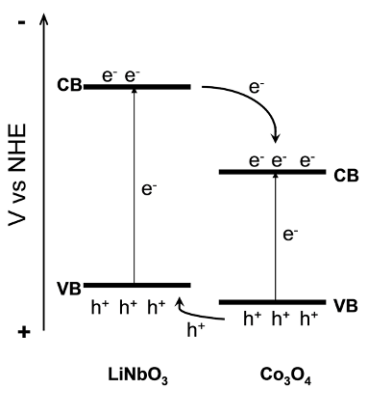

Figure 6. Proposed charge separation for $Co_3O_4/LiNbO_3$ composite under UV light irradiation.

$$E_{CB}^{0} = X - E_c - 1/2E_g \quad (1)$$

where X is the absolute electronegativity of the semiconductor expressed as the geometric mean of the absolute electronegativity of the constituent atoms, which is defined as the arithmetic mean of the atomic electron affinity and the first ionization energy. E_c is the energy of free electrons on the hydrogen scale (□4.5 eV) and E_g is the band gap of the semiconductor [20-22]. The calculated band edge positions of Co_3O_4 and $LiNbO_3$ are presented in Table 1. Fig. 6 shows the proposed charge separation process for the $Co_3O_4/LiNbO_3$ composite. From this figure it is clearly seen that both CB and VB bands of Co_3O_4 are situated below the CB and VB

Table 1. Absolute electronegativity, estimated band gap energy, energy levels of calculated conduction and valence bands for Co_3O_4 and $LiNbO_3$.

Photocatalyst	Absolute electronegativity X	Bang gap energy Eg (eV)	Calculated conduction band edge (eV)	Calculated valence band edge (eV)
Co_3O_4 [20,22]	5.903	2.07	0.37	2.44
$LiNbO_3$	4.797	3.86	-1.63	2.23

bands of $LiNbO_3$. The CB and VB position of Co_3O_4 below the CB and VB of $LiNbO_3$ permits the transfer of electrons from CB of $LiNbO_3$ to CB of Co_3O_4 and transfer of holes from VB of Co_3O_4 to VB of $LiNbO_3$. This efficient electron and hole transfer can inhibit the rapid recombination of electron-hole pairs, leading to higher activity of $Co_3O_4/LiNbO_3$ composites for photocatalytic hydrogen production. Moreover, the positive effect of the Co loading is possibly due to the higher electronegativity of Co (1.88) as compared to that of Nb (1.60), resulting in easier photoexcited electron transfer from $LiNbO_3$ conduction band to the Co species. It is possible that Co species works as active sites for proton reduction [8]. The inset in Fig. 5 shows the effect of the Co content in composites on the H_2 evolution rate. As can be seen from this figure, the Co content has a significant influence on the photocatalytic activity of composites. The amount of the H_2 released increases with the increasing content of Co from 0.5 wt.% (1.84 μmol min^{-1}) to 3 wt.% (2.59 μmol min^{-1}). Further increase of Co content to 4 wt.% leads to decrease in H_2 production (1.89 μmol min^{-1}). This effect can be explained by the partial blockage of the $LiNbO_3$ surface active sites due to excessive amount of Co_3O_4 [24]. Moreover, it is possible that at high Co content, the Co_3O_4 would tend to aggregate into larger particles which results in a negative impact on $Co_3O_4/LiNbO_3$ composite activity [22,25]. The optimum Co content in $Co_3O_4/LiNbO_3$ composite is 3 wt.%. Compared with pure $LiNbO_3$, the 3wt%-Co/$LiNbO_3$ composite exhibits double enhancement of H_2 production.

4. Conclusion

In summary, characterization and photocatalytic activity of pure $LiNbO_3$ and $Co_3O_4/LiNbO_3$ composites in a reaction of photocatalytic hydrogen generation have been presented. A clear enhancement of photoactivity of $Co_3O_4/LiNbO_3$ composites as compared to $LiNbO_3$ has been shown. Effect of Co content on photocatalytic H_2 evolution was investigated. The highest H_2 evolution efficiency was observed for $Co_3O_4/LiNbO_3$ composite with 3 wt.% cobalt content. Compared with pure $LiNbO_3$, the 3wt%-Co/$LiNbO_3$ composite exhibits double enhancement of H_2 production.

References

[1] Z. Chen et al., RSC Advances 2, 7380 (2012)
[2] L. Hao et al., Appl. Phys. Lett. 95, 232907 (2009)
[3] Q.Y. Chen et al., Trans. Nonferrous. Met. Soc. China 14, 798 (2004)
[4] K. Saito, K. Koga, A. Kudo, Dalton Trans. 40, 3909 (2011)
[5] B. Zielińska, E. Borowiak-Palen, R.J. Kalenczuk, J. Phys. Chem. Solids 69, 236 (2008)
[6] M. Stock, S. Dunn, J. Phys. Chem. C. 116, 20854 (2012)
[7] Y. Chen, H. Yang, X. Liu, L. Guo, Int. J. Hydrogen Energy 35, 7029 (2010)
[8] T. Puangpetch, T. Sreethawong, S. Chavadej, Int. J. Hydrogen Energy 35, 6531 (2010)
[9] K. Domen, A. Kudo, T. Onishi, N. Kosugi, H. Kuroda, J. Phys. Chem. 90, 292 (1986)
[10] J. Ye, Z. Zou, A. Matsushita, Int. J. Hydrogen Energy 28, 651 (2003)
[11] A. Kudo, Int. J. Hydrogen Energy 31, 197 (2006)
[12] Z. Zou, J. Ye, H. Arakawa, Int. J. Hydrogen Energy 28, 663 (2003)
[13] V.G. Hadjiev, M.N. Iliev, I.V. Vergilov, J. Phys. Solid State Phys 21, 199 (1988)
[14] F. Gu, C. Li, Y. Hu, L. Zhang, J. Crystal Growth 304, 369 (2007)
[15] M. Christy, M.R. Jisha, A. R. Kim, K.S. Nahm, D. J. Yoo, et al., Bull. Korean Chem. Soc. 32, 1204 (2011)
[16] Ch-W. Tang, Ch-B. Wang, S-H. Chien, Thermochim. Acta. 437, 68 (2008)
[17] D. Tiwari, S. Dunn, Mater Lett 79, 18 (2012)
[18] L.Z. Hao et al., Chin. Phys. Phys. Lett. 28, 107703 (2011)
[19] A. Fernández-Osorio, A.Vázquez-Olmos, R. Sato-Berru, R. Escudero, Rev. Adv. Mater. Sci. 22, 60 (2009)
[20] Q. Xiao, J. Zhang, C. Xiao, X. Tan, Catal. Commun. 9, 1247 (2008)

[21] P. Shukla, H. Sun, S. Wang, H.M. Ang, M.O. Tadé, Sep. Purif .Technol. 77, 230 (2011)
[22] M. Long, W. Cai, J. Cai, B. Zhou, X. Chai, Y. Wu, J. Phys. Chem. B. 110, 20211 (2006)
[23] Y. He, L. Zhao, Y. Wang, H. Lin, T. Li, X. Wuc, Ying Wu, Chem. Eng. J. 169, 50 (2011)
[24] J. Yu, Y. Hai, M. Jaroniec, J. Colloid. Interf. Sci. 257, 223 (2011)
[25] P.D. Tran, L. Xi, S.K. Batabyal, L.H. Wong, J. Barber, J.S.Ch. Loo, Phys. Chem. Chem. Phys. 14, 11596 (2012)